A quasi-3D theory for vibration and buckling of functionally graded sandwich beams

Thuc P. Vo[a,*], Huu-Tai Thai[b], Trung-Kien Nguyen[c], Fawad Inam[a], Jaehong Lee[d]

[a] *Faculty of Engineering and Environment, Northumbria University, Newcastle upon Tyne, NE1 8ST, UK.*
[b] *School of Civil and Environmental Engineering, The University of New South Wales, NSW 2052, Australia.*
[c] *Faculty of Civil Engineering and Applied Mechanics, University of Technical Education Ho Chi Minh City, 1 Vo Van Ngan Street, Thu Duc District, Ho Chi Minh City, Vietnam*
[d] *Department of Architectural Engineering, Sejong University 98 Kunja Dong, Kwangjin Ku, Seoul 143-747, Korea.*

Abstract

This paper presents a finite element model for free vibration and buckling analyses of functionally graded (FG) sandwich beams by using a quasi-3D theory in which both shear deformation and thickness stretching effects are included. Sandwich beams with FG skins-homogeneous core and homogeneous skins-FG core are considered. By using the Hamilton's principle, governing equations of motion for coupled axial-shear-flexural-stretching response are derived. The resulting coupling is referred to as fourfold coupled vibration and buckling. Numerical examples are carried out to investigate the thickness stretching effect on natural frequencies and critical buckling loads as well as mode shapes of sandwich beams for various power-law indexes, skin-core-skin thickness ratios and boundary conditions.

Keywords: FG sandwich beams; vibration; buckling; finite element; quasi-3D theory

1. Introduction

In recent years, there is a rapid increase in the use of functionally graded (FG) sandwich structures in aerospace, marine and civil engineering due to high strength-to-weight ratio. With the wide application of these structures, more accurate theories are required to predict their vibration and buckling response. Amirani et al. [1] used the element free Galerkin method to study free vibration analysis of sandwich beam with FG core. Bui et al. [2] investigated transient responses and natural frequencies of sandwich beams with FG core. Vo et al. [3] studied vibration and buckling of sandwich beams with FG skins - homogeneous core using a refined shear deformation theory. It should be noted

*Corresponding author, tel.: +44 191 243 7856
Email address: thuc.vo@northumbria.ac.uk (Thuc P. Vo)

that the above mentioned studies ([1]-[3]) neglected the thickness stretching effect, which becomes very important for thick plates [4]. In order to include shear deformation and thickness stretching effects, the quasi-3D theories, which are based on a higher-order variation through the thickness of the in-plane and transverse displacements, are used. By using these theories, although a lot of work has been done for isotropic and sandwich FG plates ([5]-[14]), the research on FG sandwich beams is limited. Carrera et al. [15] developed Carrera Unified Formulation (CUF) using various refined beam theories (polynomial, trigonometric, exponential and zig-zag), in which non-classical effects including the stretching effect were automatically taken into account. Recently, he and his co-workers also used CUF to investigate the free vibration of laminated beam [16] and FG layered beams [17]. As far as authors are aware, there is no work available using the quasi-3D theories to study vibration and buckling of FG sandwich beams in a unitary manner. This complicated problem is not well-investigated and there is a need for further studies.

In this paper, which improves the previous research [3] by including the thickness stretching effect, a finite element model for free vibration and buckling analyses of FG sandwich beams by using a quasi-3D theory is presented. Sandwich beams with FG skins-homogeneous core and homogeneous skins-FG core are considered. Governing equations of motion are derived by using the Hamilton's principle. A two-noded C^1 beam element with six degree-of-freedom per node is developed. Numerical examples are carried out to investigate the thickness stretching effect on natural frequencies and critical buckling loads as well as mode shapes of sandwich beams for various power-law indexes, skin-core-skin thickness ratios and boundary conditions.

2. Theoretical Formulation

2.1. FG sandwich beams

Consider a FG sandwich beam with length L and rectangular cross-section $b \times h$, with b being the width and h being the height. For simplicity, Poisson's ratio ν, is assumed to be constant. Young's modulus E and mass density ρ are expressed by [18]:

$$E(z) = (E_c - E_m)V_c + E_m \tag{1a}$$

$$\rho(z) = (\rho_c - \rho_m)V_c + \rho_m \tag{1b}$$

where subscripts m and c represent the metallic and ceramic constituents, V_c is volume fraction of the ceramic phase of the beam. Two types of FG sandwich beams are considered:

2.1.1. Type A: sandwich beam with FG skins - homogeneous core

The bottom and top skin is composed of a FG material, while, the core is ceramic (Fig. 1a). For Type A, V_c is obtained as:

$$\begin{cases} V_c = \left(\frac{z-h_o}{h_1-h_0}\right)^k, & z \in [-h/2, h_1] \quad \text{(bottom skin)} \\ V_c = 1, & z \in [h_1, h_2] \quad \text{(core)} \\ V_c = \left(\frac{z-h_3}{h_2-h_3}\right)^k, & z \in [h_2, h/2] \quad \text{(top skin)} \end{cases} \tag{2}$$

where k is the power-law index.

2.1.2. Type B: sandwich beam with homogeneous skins - FG core

The bottom and top skin is metal and ceramic, while, the core is composed of a FG material (Fig. 1b). For Type B, V_c is obtained as:

$$\begin{cases} V_c = 0, & z \in [-h/2, h_1] \quad \text{(bottom skin)} \\ V_c = \left(\frac{z-h_1}{h_2-h_1}\right)^k, & z \in [h_1, h_2] \quad \text{(core)} \\ V_c = 1, & z \in [h_2, h/2] \quad \text{(top skin)} \end{cases} \tag{3}$$

2.2. Constitutive Equations

The linear constitutive relations are given as:

$$\begin{Bmatrix} \sigma_x \\ \sigma_z \\ \sigma_{xz} \end{Bmatrix} = \begin{bmatrix} \bar{C}^*_{11} & \bar{C}^*_{13} & 0 \\ \bar{C}^*_{13} & \bar{C}^*_{11} & 0 \\ 0 & 0 & C_{55} \end{bmatrix} \begin{Bmatrix} \epsilon_x \\ \epsilon_z \\ \gamma_{xz} \end{Bmatrix} \tag{4}$$

where

$$\bar{C}^*_{11} = \bar{C}_{11} - \frac{\bar{C}^2_{12}}{\bar{C}_{22}} = \frac{E(z)}{1-\nu^2} \tag{5a}$$

$$\bar{C}^*_{13} = \bar{C}_{13} - \frac{\bar{C}_{12}\bar{C}_{23}}{\bar{C}_{22}} = \frac{E(z)\nu}{1-\nu^2} \tag{5b}$$

$$C_{55} = \frac{E(z)}{2(1+\nu)} \tag{5c}$$

If the thickness stretching effect is omitted ($\epsilon_z = 0$), elastic constants C_{ij} in Eq. (5) are reduced as:

$$\bar{C}^*_{11} = E(z) \tag{6a}$$

$$\bar{C}^*_{13} = 0 \tag{6b}$$

$$C_{55} = \frac{E(z)}{2(1+\nu)} \tag{6c}$$

2.3. Kinematics

This paper extends a refined shear deformation theory from previous research [3] by including the thickness stretching effect. The new displacement field is assumed to be [19]:

$$U(x,z,t) = u(x,t) - z\frac{\partial w_b(x,t)}{\partial x} - \frac{4z^3}{3h^2}\frac{\partial w_s(x,t)}{\partial x} = u(x,t) - zw'_b(x,t) - f(z)w'_s(x,t) \tag{7a}$$

$$W(x,z,t) = w_b(x,t) + w_s(x,t) + (1 - \frac{4z^2}{h^2})w_z(x,t) = w_b(x,t) + w_s(x,t) + g(z)w_z(x,t) \tag{7b}$$

where u, w_b, w_s and w_z are four unknown displacements of mid-plane of the beam. It should be noted that the new component $g(z)w_z(x,t)$ in Eq. (7b) is added to investigate the thickness stretching effect on the vibration and buckling of FG sandwich beams.

The only non-zero strains are:

$$\epsilon_x = \frac{\partial U}{\partial x} = u' - zw''_b - fw''_s \tag{8a}$$

$$\epsilon_z = \frac{\partial W}{\partial z} = g'w_z \tag{8b}$$

$$\gamma_{xz} = \frac{\partial W}{\partial x} + \frac{\partial U}{\partial z} = g(w'_s + w'_z) \tag{8c}$$

2.4. Variational Formulation

The variation of the strain energy can be stated as:

$$\begin{aligned}\delta\mathcal{U} &= \int_0^l \int_0^b \left[\int_{-h/2}^{h/2} (\sigma_x \delta\epsilon_x + \sigma_{xz}\delta\gamma_{xz} + \sigma_z g'\delta w_z)dz \right] dydx \\ &= \int_0^l \left[N_x\delta u' - M^b_x\delta w''_b - M^s_x\delta w''_s + Q_{xz}(\delta w'_s + \delta w'_z) + R_z\delta w_z \right])dx \end{aligned} \tag{9}$$

where $N_x, M^b_x, M^s_x, Q_{xz}$ and R_z are the stress resultants, defined as:

$$N_x = \int_{-h/2}^{h/2} \sigma_x b dz \tag{10a}$$

$$M^b_x = \int_{-h/2}^{h/2} \sigma_x z b dz \tag{10b}$$

$$M^s_x = \int_{-h/2}^{h/2} \sigma_x f b dz \tag{10c}$$

$$Q_{xz} = \int_{-h/2}^{h/2} \sigma_{xz} g b dz \tag{10d}$$

$$R_z = \int_{-h/2}^{h/2} \sigma_z g' b dz \tag{10e}$$

The variation of the potential energy by the axial force P_0 can be written as:

$$\delta\mathcal{V} = -\int_0^l P_0 \Big[\delta w_b'(w_b' + w_s') + \delta w_s'(w_b' + w_s')\Big] dx \tag{11}$$

The variation of the kinetic energy can be expressed as:

$$\begin{aligned}
\delta\mathcal{K} &= \int_0^l \int_0^b \left[\int_{-h/2}^{h/2} \rho(\dot{U}\delta\dot{U} + \dot{W}\delta\dot{W}) dz\right] dy dx \\
&= \int_0^l \Big[\delta\dot{u}(m_0\dot{u} - m_1\dot{w}_b{}' - m_f\dot{w}_s{}') + \delta\dot{w}_b[m_0(\dot{w}_b + \dot{w}_s) + m_g\dot{w}_z] + \delta\dot{w}_b{}'(-m_1\dot{u} + m_2\dot{w}_b{}' + m_{fz}\dot{w}_s{}') \\
&+ \delta\dot{w}_s[m_0(\dot{w}_b + \dot{w}_s) + m_g\dot{w}_z] + \delta\dot{w}_s{}'(-m_f\dot{u} + m_{fz}\dot{w}_b{}' + m_{f^2}\dot{w}_s{}') \\
&+ \delta\dot{w}_z[m_g(\dot{w}_b + \dot{w}_s) + m_{g^2}\dot{w}_z]\Big] dx
\end{aligned} \tag{12}$$

where

$$(m_0, m_1, m_2) = \int_{-h/2}^{h/2} \rho(1, z, z^2) b dz \tag{13a}$$

$$(m_f, m_{fz}, m_{f^2}) = \int_{-h/2}^{h/2} \rho(f, fz, f^2) b dz \tag{13b}$$

$$(m_g, m_{g^2}) = \int_{-h/2}^{h/2} \rho(g, g^2) b dz \tag{13c}$$

By using Hamilton's principle, the following weak statement is obtained:

$$\begin{aligned}
0 &= \int_{t_1}^{t_2} (\delta\mathcal{K} - \delta\mathcal{U} - \delta\mathcal{V}) dt \\
0 &= \int_{t_1}^{t_2} \int_0^l \Big[\delta\dot{u}(m_0\dot{u} - m_1\dot{w}_b{}' - m_f\dot{w}_s{}') + \delta\dot{w}_b[m_0(\dot{w}_b + \dot{w}_s) + m_g\dot{w}_z] + \delta\dot{w}_b{}'(-m_1\dot{u} + m_2\dot{w}_b{}' + m_{fz}\dot{w}_s{}') \\
&+ \delta\dot{w}_s[m_0(\dot{w}_b + \dot{w}_s) + m_g\dot{w}_z] + \delta\dot{w}_s{}'(-m_f\dot{u} + m_{fz}\dot{w}_b{}' + m_{f^2}\dot{w}_s{}') + \delta\dot{w}_z[m_g(\dot{w}_b + \dot{w}_s) + m_{g^2}\dot{w}_z] \\
&+ P_0\big[\delta w_b'(w_b' + w_s') + \delta w_s'(w_b' + w_s')\big] - N_x\delta u' + M_x^b\delta w_b'' + M_x^s\delta w_s'' - Q_{xz}\delta w_s' - R_z\delta w_z\Big] dx dt
\end{aligned} \tag{14}$$

2.5. Governing Equations of Motion

By integrating Eq. (14) by parts and collecting the coefficients of $\delta u, \delta w_b$, δw_s and δw_z, the governing equations of motion can be obtained:

$$N_x' = m_0\ddot{u} - m_1\ddot{w}_b{}' - m_f\ddot{w}_s{}' \tag{15a}$$

$$M_x^{b\prime\prime} - P_0(w_b'' + w_s'') = m_0(\ddot{w}_b + \ddot{w}_s) + m_1\ddot{u}' - m_2\ddot{w}_b{}'' - m_{fz}\ddot{w}_s{}'' + m_g\ddot{w}_z \tag{15b}$$

$$M_x^{s\prime\prime} + Q_{xz}' - P_0(w_b'' + w_s'') = m_0(\ddot{w}_b + \ddot{w}_s) + m_f\ddot{u}' - m_{fz}\ddot{w}_b{}'' - m_{f^2}\ddot{w}_s{}'' + m_g\ddot{w}_z \tag{15c}$$

$$Q_{xz}' - R_z = m_g(\ddot{w}_b + \ddot{w}_s) + m_{g^2}\ddot{w}_z \tag{15d}$$

By substituting Eqs. (4) and (8) into Eq. (10), the stress resultants can be expressed in term of displacements:

$$\begin{Bmatrix} N_x \\ M_x^b \\ M_x^s \\ R_z \\ Q_{xz} \end{Bmatrix} = \begin{bmatrix} A & B & B_s & X & 0 \\ & D & D_s & Y & 0 \\ & & H & Y_s & 0 \\ & & & Z & 0 \\ sym. & & & & A_s \end{bmatrix} \begin{Bmatrix} u' \\ -w_b'' \\ -w_s'' \\ w_z \\ w_s' + w_z' \end{Bmatrix} \tag{16}$$

where

$$(A, B, B_s, D, D_s, H, Z) = \int_{-h/2}^{h/2} \bar{C}_{11}^*(1, z, f, z^2, fz, f^2, g'^2) b dz \tag{17a}$$

$$A_s = \int_{-h/2}^{h/2} C_{55} g^2 b dz \tag{17b}$$

$$(X, Y, Y_s) = \int_{-h/2}^{h/2} \bar{C}_{13}^* g'(1, z, f) b dz \tag{17c}$$

By substituting Eq. (16) into Eq. (15), the governing equations of motion can be expressed in term of displacements:

$$Au'' - Bw_b''' - B_s w_s''' + Xw_z' = m_0\ddot{u} - m_1\ddot{w}_b{}' - m_f\ddot{w}_s{}' \tag{18a}$$

$$\begin{aligned} Bu''' - Dw_b^{iv} - D_s w_s^{iv} + Yw_z'' - P_0(w_b'' + w_s'') &= m_1\ddot{u}' + m_0(\ddot{w}_b + \ddot{w}_s) - m_2\ddot{w}_b{}'' \\ &- m_{fz}\ddot{w}_s{}'' + m_g\ddot{w}_z \end{aligned} \tag{18b}$$

$$\begin{aligned} B_s u''' - D_s w_b^{iv} - Hw_s^{iv} + A_s w_s'' + (A_s + Y_s)w_z'' - P_0(w_b'' + w_s'') &= m_f\ddot{u}' + m_0(\ddot{w}_b + \ddot{w}_s) - m_{fz}\ddot{w}_b{}'' \\ &- m_{f^2}\ddot{w}_s{}'' + m_g\ddot{w}_z \end{aligned} \tag{18c}$$

$$-Xu' + Yw_b'' + (A_s + Y_s)w_s'' + A_s w_z'' - Zw_z = m_g(\ddot{w}_b + \ddot{w}_s) + m_{g^2}\ddot{w}_z \tag{18d}$$

3. Finite Element Formulation

A two-noded C^1 beam element with six degree-of-freedom per node is developed. Linear polynomial Ψ_j is used for u and w_z and Hermite-cubic polynomial ψ_j is used for w_b and w_s. The generalized displacements within an element are expressed as:

$$u = \sum_{j=1}^{2} u_j \Psi_j \tag{19a}$$

$$w_b = \sum_{j=1}^{4} w_{bj}\psi_j \tag{19b}$$

$$w_s = \sum_{j=1}^{4} w_{sj}\psi_j \tag{19c}$$

$$w_z = \sum_{j=1}^{2} w_{zj}\Psi_j \tag{19d}$$

By substituting Eq. (19) into Eq. (14), the finite element model of a typical element can be expressed:

$$([K] - P_0[G] - \omega^2[M])\{\Delta\} = \{0\} \tag{20}$$

where the explicit forms of element stiffness matrix $[K]$, geometric stiffness $[G]$ and mass matrix $[M]$ are given by:

$$K_{ij}^{11} = \int_0^l A\Psi_i'\Psi_j' dx \tag{21a}$$

$$K_{ij}^{12} = -\int_0^l B\Psi_i'\psi_j'' dx \tag{21b}$$

$$K_{ij}^{13} = -\int_0^l B_s\Psi_i'\psi_j'' dx \tag{21c}$$

$$K_{ij}^{14} = \int_0^l X\Psi_i'\Psi_j dx \tag{21d}$$

$$K_{ij}^{22} = \int_0^l D\psi_i''\psi_j'' dx \tag{21e}$$

$$K_{ij}^{23} = \int_0^l D_s\psi_i''\psi_j'' dx \tag{21f}$$

$$K_{ij}^{24} = -\int_0^l Y\psi_i''\Psi_j dx \tag{21g}$$

$$K_{ij}^{33} = \int_0^l (H\psi_i''\psi_j'' + A_s\psi_i'\psi_j') dx \tag{21h}$$

$$K_{ij}^{34} = \int_0^l (-Y_s\psi_i''\Psi_j + A_s\psi_i'\Psi_j') dx \tag{21i}$$

$$K_{ij}^{44} = \int_0^l (Z\Psi_i\Psi_j + A_s\Psi_i'\Psi_j') dx \tag{21j}$$

$$G_{ij}^{22} = \int_0^l \psi_i'\psi_j' dx \tag{21k}$$

$$G_{ij}^{23} = \int_0^l \psi_i'\psi_j' dx \tag{21l}$$

$$G_{ij}^{33} = \int_0^l \psi_i'\psi_j' dx \tag{21m}$$

$$M_{ij}^{11} = \int_0^l m_0 \Psi_i \Psi_j dx \tag{21n}$$

$$M_{ij}^{12} = -\int_0^l m_1 \Psi_i \psi_j' dx \tag{21o}$$

$$M_{ij}^{13} = -\int_0^l m_f \Psi_i \psi_j' dx \tag{21p}$$

$$M_{ij}^{22} = \int_0^l (m_0 \psi_i \psi_j + m_2 \psi_i' \psi_j') dx \tag{21q}$$

$$M_{ij}^{23} = \int_0^l (m_0 \psi_i \psi_j + m_{fz} \psi_i' \psi_j') dx \tag{21r}$$

$$M_{ij}^{24} = \int_0^l m_g \psi_i \Psi_j dx \tag{21s}$$

$$M_{ij}^{33} = \int_0^l (m_0 \psi_i \psi_j + m_{f^2} \psi_i' \psi_j') dx \tag{21t}$$

$$M_{ij}^{34} = \int_0^l m_g \psi_i \Psi_j dx \tag{21u}$$

$$M_{ij}^{44} = \int_0^l m_{g^2} \Psi_i \Psi_j dx \tag{21v}$$

In Eq. (20), $\{\Delta\}$ is the eigenvector of nodal displacements corresponding to an eigenvalue:

$$\{\Delta\} = \{u \; w_b \; w_s \; w_z\}^{\mathrm{T}} \tag{22}$$

4. Numerical Examples

In this section, FG sandwich beams with various configurations are analysed and compared results with the available solutions to verify the accuracy of the proposed theory and investigate the thickness stretching effect on their vibration and buckling response. Unless mentioned otherwise, FG sandwich beams with slenderness ratio $L/h = 5$ and 20, whose material properties are: Aluminum as metal (Al: $E_m = 70\text{GPa}, \nu_m = 0.3, \rho_m = 2702\text{kg/m}^3$) and Alumina as ceramic (Al_2O_3: $E_c = 380\text{GPa}, \nu_c = 0.3, \rho_c = 3960\text{kg/m}^3$), are considered. The following non-dimensional parameters are used:

$$\overline{\omega} = \frac{\omega L^2}{h}\sqrt{\frac{\rho_m}{E_m}} \tag{23a}$$

$$\overline{P}_{cr} = P_{cr}\frac{12L^2}{E_m h^3} \tag{23b}$$

4.1. FG beams

As the first example, the results of FG beams computed by the present theory are compared with those obtained using the first-order beam theory (FOBT) of Li and Batra [20] and Nguyen et al. [21] and the higher-order beam theory (HOBT) of Vo et al. [3], Simsek [22] and Thai and Vo [23]. It

should be noted that Li and Batra [20] used $\nu_m = \nu_c = 0.23$. Comparisons are given in Tables 1 and 2 for FG beams with various configurations. A good agreement between present results and previous solutions can be observed. It can be seen that the results from FOBT and HOBT due to ignoring the thickness stretching effect ($\epsilon_z = 0$) are slightly underestimate when comparing with those from the present theory (quasi-3D, $\epsilon_z \neq 0$). This effect is more pronounced on thick beams ($L/h = 5$) and is a little greater for clamped-clamped (C-C) beams as compared with simply-supported (S-S) and clamped-free (C-F) ones.

4.2. FG sandwich beams

In order to demonstrate the validity of the present model further, a cantilever sandwich beam with L=200 mm and cross-section 20 mm×20 mm is considered. The core with the thickness $t_c = 14$ mm is made of Aluminum and Zirconia (Al/ZrO_2) and faces with the thickness $t_f = 3$ mm are made of Steel (Fe), whose material properties are: Al ($E_m = 70\text{GPa}, \nu_m = 0.3, \rho_m = 2700\text{kg/m}^3$) and ZrO_2 ($E_c = 151\text{GPa}, \nu_c = 0.3, \rho_c = 5700\text{kg/m}^3$) and Fe ($E_f = 210\text{GPa}, \nu_f = 0.3, \rho_f = 7860\text{kg/m}^3$). The first five natural frequencies are given in Table 3 along with results of Bui et al. [2] using 3D finite element model (ANSYS) and meshfree method as well as of Mashat et al. [17] using the Carrera Unified Formulation ($TE8^{zz}$ and $E4\text{-}4_2$). It can be seen that the solutions obtained from the proposed theory are in excellent agreement with those obtained from previous results, especially with CUF model, which included the stretching effect.

In the next example, Tables 4-11 give the results of sandwich beams of Type A with different skin-core-skin thickness ratios and (1-8-1) sandwich beams of Type B and compare with those using HOBT [3]. It is clear that for Type A they decrease with the increase of k and decrease of skin-core-skin thickness ratio. It can be seen again that the results with the thickness stretching effect ($\epsilon_z \neq 0$) are higher than those without it ($\epsilon_z = 0$). As the span-to-height ratio increases, these differences decrease, which can be predicted since the thick beams sketch more in thickness direction. Moreover, Type B beams are slightly more sensitive than Type A even for $L/h = 20$, especially for buckling results (Table 11). The buckling mode shapes of sandwich beams of Type B with various power-law indexes ($k = 0, 1$ and 10) using HOBT and present theory are illustrated in Fig. 2. Due to coupling from thickness stretching effect, they are slightly different. For HOBT, when the beam is buckling exhibits triply coupled mode (u, w_b and w_s), whereas, for quasi-3D theory, it displays fourfold coupled mode (u, w_b, w_s and w_z). Fig. 3 plots the natural frequencies and critical buckling loads versus slenderness ratio of (1-0-1) and (1-8-1) sandwich beams of Type A. Due to core layer, the effect of k on (1-8-1) sandwich beams is smaller than that of (1-0-1) ones. As expected, the bottom and top curves correspond to metal beams and ceramic ones.

Finally, the first fourth natural frequencies of (2-1-1) sandwich beams of Type A and B are given in Tables 12 and 13. As expected, the results from HOBT are smaller than those from the present theory. In Figs. 4 and 5, the first four vibration modes of sandwich beams with $k = 1$ is presented. It can be seen that all vibration mode shapes show fourfold coupled mode (axial-shear-flexural-sketching) for present theory and triply coupled (axial-shear-flexural) mode for HOBT. It is from this fourfold coupled mode that highlights the effect of thickness stretching on the vibration and buckling of sandwich beams. This mode is never seen in the HOBT [3] because the thickness stretching effect is not present. It confirms again that this effect is important and should be considered in analysis of thick and moderately thick sandwich beams.

5. Conclusions

A finite element model based on a quasi-3D theory is presented to study the free vibration and buckling analyses of FG sandwich beams. Sandwich beams with FG skins-homogeneous core and homogeneous skins-FG core are considered. This model can predict accurately the natural frequencies and critical buckling loads as well as corresponding mode shapes of sandwich beams for various configuration. Fourfold coupled (axial-shear-flexural-stretching) vibration and buckling mode is observed. The thickness stretching effect is important and should be considered in analysis of thick and moderately thick sandwich beams.

6. Acknowledgements

The authors gratefully acknowledges research support fund from UoA16 by Northumbria University and by the Basic Research Laboratory Program of the National Research Foundation of Korea (NRF) funded by the Ministry of Education, Science and Technology (2010-0019373 and 2012R1A2A1A01007450).

References

References

[1] M. C. Amirani, S. M. R. Khalili, N. Nemati, Free vibration analysis of sandwich beam with FG core using the element free Galerkin method, Composite Structures 90 (3) (2009) 373 – 379.

[2] T. Q. Bui, A. Khosravifard, C. Zhang, M. R. Hematiyan, M. V. Golub, Dynamic analysis of sandwich beams with functionally graded core using a truly meshfree radial point interpolation method, Engineering Structures 47 (0) (2013) 90 – 104.

[3] T. P. Vo, H.-T. Thai, T.-K. Nguyen, A. Maheri, J. Lee, Finite element model for vibration and buckling of functionally graded sandwich beams based on a refined shear deformation theory, Engineering Structures 64 (0) (2014) 12 – 22.

[4] E. Carrera, S. Brischetto, M. Cinefra, M. Soave, Effects of thickness stretching in functionally graded plates and shells, Composites Part B: Engineering 42 (2) (2011) 123 – 133.

[5] A. M. Zenkour, Benchmark trigonometric and 3-D elasticity solutions for an exponentially graded thick rectangular plate, Archive of Applied Mechanics 77 (4) (2007) 197–214.

[6] A. M. A. Neves, A. J. M. Ferreira, E. Carrera, M. Cinefra, R. M. N. Jorge, C. M. M. Soares, Buckling analysis of sandwich plates with functionally graded skins using a new quasi-3D hyperbolic sine shear deformation theory and collocation with radial basis functions, ZAMM - Journal of Applied Mathematics and Mechanics 92 (9) (2012) 749–766.

[7] A. M. A. Neves, A. J. M. Ferreira, E. Carrera, C. M. C. Roque, M. Cinefra, R. M. N. Jorge, C. M. M. Soares, A quasi-3D sinusoidal shear deformation theory for the static and free vibration analysis of functionally graded plates, Composites Part B: Engineering 43 (2) (2012) 711 – 725.

[8] A. M. A. Neves, A. J. M. Ferreira, E. Carrera, M. Cinefra, C. M. C. Roque, R. M. N. Jorge, C. M. M. Soares, A quasi-3D hyperbolic shear deformation theory for the static and free vibration analysis of functionally graded plates , Composite Structures 94 (5) (2012) 1814 – 1825.

[9] A. M. A. Neves, A. J. M. Ferreira, E. Carrera, M. Cinefra, C. M. C. Roque, R. M. N. Jorge, C. M. M. Soares, Static, free vibration and buckling analysis of isotropic and sandwich functionally graded plates using a quasi-3D higher-order shear deformation theory and a meshless technique, Composites Part B: Engineering 44 (1) (2013) 657 – 674.

[10] J. L. Mantari, C. G. Soares, Generalized hybrid quasi-3D shear deformation theory for the static analysis of advanced composite plates , Composite Structures 94 (8) (2012) 2561 – 2575.

[11] J. L. Mantari, C. G. Soares, A novel higher-order shear deformation theory with stretching effect for functionally graded plates, Composites Part B: Engineering 45 (1) (2013) 268 – 281.

[12] H.-T. Thai, T. P. Vo, T. Q. Bui, T.-K. Nguyen, A quasi-3D hyperbolic shear deformation theory for functionally graded plates, Acta Mechanica (2013) 1–14.

[13] H.-T. Thai, S.-E. Kim, A simple quasi-3D sinusoidal shear deformation theory for functionally graded plates , Composite Structures 99 (0) (2013) 172 – 180.

[14] H.-T. Thai, D.-H. Choi, Improved refined plate theory accounting for effect of thickness stretching in functionally graded plates, Composites Part B: Engineering 56 (0) (2014) 705 – 716.

[15] E. Carrera, G. Giunta, M. Petrolo, Beam structures: classical and advanced theories, John Wiley & Sons, 2011.

[16] E. Carrera, M. Filippi, E. Zappino, Free vibration analysis of laminated beam by polynomial, trigonometric, exponential and zig-zag theories, Journal of Composite Materials, 48 (19) (2014) 2299 – 2316.

[17] D. S. Mashat, E. Carrera, A. M. Zenkour, S. A. A. Khateeb, M. Filippi, Free vibration of FGM layered beams by various theories and finite elements, Composites Part B: Engineering 59 (0) (2014) 269 – 278.

[18] J. N. Reddy, Mechanics of laminated composite plates and shells: theory and analysis, CRC, 2004.

[19] J. N. Reddy, A simple higher-order theory for laminated composite plates, Journal of Applied Mechanics 51 (4) (1984) 745–752.

[20] S.-R. Li, R. C. Batra, Relations between buckling loads of functionally graded Timoshenko and homogeneous Euler-Bernoulli beams, Composite Structures 95 (0) (2013) 5 – 9.

[21] T.-K. Nguyen, T. P. Vo, H.-T. Thai, Static and free vibration of axially loaded functionally graded beams based on the first-order shear deformation theory, Composites Part B: Engineering 55 (0) (2013) 147–157.

[22] M. Simsek, Fundamental frequency analysis of functionally graded beams by using different higher-order beam theories, Nuclear Engineering and Design 240 (4) (2010) 697 – 705.

[23] H.-T. Thai, T. P. Vo, Bending and free vibration of functionally graded beams using various higher-order shear deformation beam theories, International Journal of Mechanical Sciences 62 (1) (2012) 57–66.

Figure 1: Geometry and coordinate of a FG sandwich beam.

Figure 2: Buckling mode shapes of (1-8-1) clamped- clamped FG sandwich beam (Type B, L/h=5).

Figure 3: Fundamental natural frequencies and critical buckling loads of (1-0-1) and (1-8-1) simply-supported FG sandwich beams (Type A).

Figure 4: Vibration mode shapes of (2-1-1) simply-supported FG sandwich beam (Type A, k=1, L/h=5).

Figure 5: Vibration mode shapes of (2-1-1) clamped-clamped FG sandwich beam (Type B, k=1, L/h=5).

Table 1: The fundamental natural frequencies of FG beams.

Table 2: The critical buckling loads of FG beams.

Table 3: The first five natural frequencies of a cantilever sandwich beam with a FG core and isotropic faces (k=1).

Table 4: The fundamental natural frequencies of FG sandwich S-S beams (Type A).

Table 5: The fundamental natural frequencies of FG sandwich C-C beams (Type A).

Table 6: The fundamental natural frequencies of FG sandwich C-F beams (Type A).

Table 7: The critical buckling loads of FG sandwich S-S beams (Type A).

Table 8: The critical buckling loads of FG sandwich C-C beams (Type A).

Table 9: The critical buckling loads of FG sandwich C-F beams (Type A).

Table 10: The fundamental natural frequencies of FG beams (Type B).

Table 11: The critical buckling loads of 1-8-1 FG beams (Type B).

Table 12: The first four natural frequencies of (2-1-1) FG sandwich beams (Type A, $L/h = 5$).

Table 13: The first four natural frequencies of (2-1-1) FG sandwich beams (Type B, $L/h = 5$).

CAPTIONS OF TABLES

Table 1: The fundamental natural frequencies of FG beams.

BC	Reference	k = 0	k = 0.5	k = 1	k = 2	k = 5	k = 10
L/h=5							
C-C	Simsek [22] (HOBT)	10.0705	8.7467	7.9503	7.1767	6.4935	6.1652
	Vo et al. [3] (HOBT)	10.0678	8.7457	7.9522	7.1801	6.4961	6.1662
	Present (Quasi-3D)	10.1851	8.8641	8.0770	7.3039	6.5960	6.2475
S-S	Simsek [22] (HOBT)	5.1527	4.4111	3.9904	3.6264	3.4012	3.2816
	Thai & Vo [23] (HOBT)	5.1527	4.4107	3.9904	3.6264	3.4012	3.2816
	Vo et al. [3] (HOBT)	5.1528	4.4019	3.9716	3.5979	3.3743	3.2653
	Present (Quasi-3D)	5.1618	4.4240	4.0079	3.6442	3.4133	3.2903
C-F	Simsek [22] (HOBT)	1.8952	1.6182	1.4633	1.3325	1.2592	1.2183
	Vo et al. [3] (HOBT)	1.8952	1.6180	1.4633	1.3326	1.2592	1.2184
	Present (Quasi-3D)	1.9055	1.6313	1.4804	1.3524	1.2763	1.2308
L/h=20							
C-C	Simsek [22] (HOBT)	12.2238	10.4287	9.4316	8.5975	8.1446	7.8858
	Vo et al. [3] (HOBT)	12.2228	10.4279	9.4328	8.5994	8.1460	7.8862
	Present (Quasi-3D)	12.2660	10.4948	9.5277	8.7142	8.2445	7.9543
S-S	Simsek [22] (HOBT)	5.4603	4.6516	4.2050	3.8361	3.6485	3.5390
	Thai & Vo [23] (HOBT)	5.4603	4.6511	4.2051	3.8361	3.6485	3.5390
	Vo et al. [3] (HOBT)	5.4603	4.6506	4.2039	3.8343	3.6466	3.5379
	Present (Quasi-3D)	5.4610	4.6659	4.2347	3.8765	3.6824	3.5590
C-F	Simsek [22] (HOBT)	1.9495	1.6605	1.5011	1.3696	1.3033	1.2645
	Vo et al. [3] (HOBT)	1.9496	1.6603	1.5011	1.3696	1.3034	1.2645
	Present (Quasi-3D)	1.9527	1.6681	1.5139	1.3862	1.3176	1.2736

Table 2: The critical buckling loads of FG beams.

BC	Reference	k = 0	k = 0.5	k = 1	k = 2	k = 5	k = 10
L/h=5							
C-C	Li & Batra [20] (FOBT)	154.3500	103.2200	80.4980	62.6140	50.3840	44.2670
	Vo et al. [3] (HOBT)	154.5500	103.7490	80.6087	61.7925	47.7562	41.8042
	Present (Quasi-3D)	160.1070	107.6550	83.6958	64.1227	49.3856	43.1579
S-S	Nguyen et al. [21] (FOBT)	48.8350	31.9610	24.6870	19.2450	16.0240	14.4270
	Vo et al. [3] (HOBT)	48.8401	32.0094	24.6911	19.1605	15.7400	14.1468
	Present (Quasi-3D)	49.5901	32.5867	25.2116	19.6124	16.0842	14.4116
C-F	Li & Batra [20] (FOBT)	13.2130	8.5782	6.6002	5.1495	4.3445	3.9501
	Vo et al. [3] (HOBT)	13.0771	8.5020	6.5428	5.0979	4.2776	3.8821
	Present (Quasi-3D)	13.0993	8.5469	6.6067	5.1680	4.3290	3.9121
L/h=10							
C-C	Li & Batra [20] (FOBT)	195.3400	127.8700	98.7490	76.9800	64.0960	57.7080
	Vo et al. [3] (HOBT)	195.3610	128.0500	98.7868	76.6677	62.9786	56.5971
	Present (Quasi-3D)	198.7060	130.5760	101.0200	78.5783	64.4350	57.7339
S-S	Nguyen et al. [21] (FOBT)	52.3080	33.9890	26.1710	20.4160	17.1940	15.6120
	Vo et al. [3] (HOBT)	52.3082	34.0087	26.1727	20.3936	17.1118	15.5291
	Present (Quasi-3D)	52.5361	34.2724	26.4869	20.7164	17.3580	15.6895
C-F	Li & Batra [20] (FOBT)	13.2130	8.5666	6.6570	5.1944	4.3903	3.9969
	Vo et al. [3] (HOBT)	13.3137	8.6370	6.6425	5.1814	8.1791	3.9794
	Present (Quasi-3D)	13.3406	8.6855	6.7098	5.2551	4.4287	4.0130
L/h=20							
C-C	Vo et al. [3] (HOBT)	209.2330	136.0490	104.7160	81.6035	68.4689	62.1282
	Present (Quasi-3D)	210.4890	137.3160	106.1200	82.9975	69.5392	62.8546
S-S	Vo et al. [3] (HOBT)	53.2546	34.5488	26.5718	20.7275	17.4935	15.9185
	Present (Quasi-3D)	53.3075	34.7084	26.8174	21.0066	17.7048	16.0416
C-F	Vo et al. [3] (HOBT)	13.3742	8.6714	6.6680	5.2027	4.3976	4.0046
	Present (Quasi-3D)	13.3896	8.7130	6.7307	5.2736	4.4512	4.0359

Table 3: The first five natural frequencies of a cantilever sandwich beam with a FG core and isotropic faces (k=1).

Mode	Bui et al. [2]		Mashat et al. [17]		Present
	ANSYS	Meshfree	$TE8^{zz}$	$E4\text{-}4_2$	
1	459.50	459.40	461.60	461.90	460.36
2	2708.70	2708.70	2720.00	2724.30	2721.55
3	6440.80	6440.70	6455.10	6455.10	6743.00
4	6991.40	6995.80	7016.70	7035.90	7046.27
5	12446.00	12446.40	12483.00	12531.70	12582.60

Table 4: The fundamental natural frequencies of FG sandwich S-S beams (Type A).

k	Theory	1-0-1	2-1-2	2-1-1	1-1-1	2-2-1	1-2-1	1-8-1
L/h=5								
0	Vo et al. [3] (HOBT)	5.1528	5.1528	5.1528	5.1528	5.1528	5.1528	5.1528
	Present (Quasi-3D)	5.1618	5.1618	5.1618	5.1618	5.1618	5.1618	5.1618
0.5	Vo et al. [3] (HOBT)	4.1268	4.2351	4.2945	4.3303	4.4051	4.4798	4.8422
	Present (Quasi-3D)	4.1344	4.2429	4.3041	4.3383	4.4146	4.4881	4.8511
1	Vo et al. [3] (HOBT)	3.5735	3.7298	3.8187	3.8755	3.9896	4.1105	4.6795
	Present (Quasi-3D)	3.5803	3.7369	3.8301	3.8830	4.0005	4.1185	4.6884
2	Vo et al. [3] (HOBT)	3.0680	3.2365	3.3514	3.4190	3.5692	3.7334	4.5142
	Present (Quasi-3D)	3.0737	3.2427	3.3656	3.4257	3.5825	3.7410	4.5231
5	Vo et al. [3] (HOBT)	2.7446	2.8439	2.9746	3.0181	3.1928	3.3771	4.3501
	Present (Quasi-3D)	2.7493	2.8489	2.9912	3.0238	3.2087	3.3840	4.3589
10	Vo et al. [3] (HOBT)	2.6932	2.7355	2.8669	2.8808	3.0588	3.2356	4.2776
	Present (Quasi-3D)	2.6978	2.7400	2.8839	2.8860	3.0757	3.2422	4.2864
L/h=20								
0	Vo et al. [3] (HOBT)	5.4603	5.4603	5.4603	5.4603	5.4603	5.4603	5.4603
	Present (Quasi-3D)	5.4610	5.4610	5.4610	5.4610	5.4610	5.4610	5.4610
0.5	Vo et al. [3] (HOBT)	4.3148	4.4290	4.4970	4.5324	4.6170	4.6979	5.1067
	Present (Quasi-3D)	4.3153	4.4296	4.4992	4.5330	4.6190	4.6985	5.1073
1	Vo et al. [3] (HOBT)	3.7147	3.8768	3.9774	4.0328	4.1602	4.2889	4.9233
	Present (Quasi-3D)	3.7152	3.8773	3.9822	4.0333	4.1641	4.2895	4.9239
2	Vo et al. [3] (HOBT)	3.1764	3.3465	3.4754	3.5389	3.7049	3.8769	4.7382
	Present (Quasi-3D)	3.1768	3.3469	3.4838	3.5394	3.7118	3.8774	4.7388
5	Vo et al. [3] (HOBT)	2.8439	2.9310	3.0773	3.1111	3.3028	3.4921	4.5554
	Present (Quasi-3D)	2.8443	2.9314	3.0891	3.1115	3.3133	3.4926	4.5560
10	Vo et al. [3] (HOBT)	2.8041	2.8188	2.9662	2.9662	3.1613	3.3406	4.4749
	Present (Quasi-3D)	2.8045	2.8191	2.9786	2.9665	3.1732	3.3411	4.4755

Table 5: The fundamental natural frequencies of FG sandwich C-C beams (Type A).

k	Theory	1-0-1	2-1-2	2-1-1	1-1-1	2-2-1	1-2-1	1-8-1
L/h=5								
0	Vo et al. [3] (HOBT)	10.0678	10.0678	10.0678	10.0678	10.0678	10.0678	10.0678
	Present (Quasi-3D)	10.1851	10.1851	10.1851	10.1851	10.1851	10.1851	10.1851
0.5	Vo et al. [3] (HOBT)	8.3600	8.5720	8.6673	8.7423	8.8648	8.9942	9.5731
	Present (Quasi-3D)	8.4635	8.6780	8.7755	8.8498	8.9743	9.1036	9.6857
1	Vo et al. [3] (HOBT)	7.3661	7.6865	7.8390	7.9580	8.1554	8.3705	9.3076
	Present (Quasi-3D)	7.4611	7.7854	7.9431	8.0595	8.2615	8.4752	9.4174
2	Vo et al. [3] (HOBT)	6.4095	6.7826	6.9908	7.1373	7.4105	7.7114	9.0343
	Present (Quasi-3D)	6.4952	6.8740	7.0920	7.2328	7.5143	7.8114	9.1415
5	Vo et al. [3] (HOBT)	5.7264	6.0293	6.2737	6.3889	6.7188	7.0691	8.7605
	Present (Quasi-3D)	5.8016	6.1124	6.3718	6.4780	6.8210	7.1652	8.8653
10	Vo et al. [3] (HOBT)	5.5375	5.8059	6.0527	6.1240	6.4641	6.8087	8.6391
	Present (Quasi-3D)	5.6074	5.8848	6.1485	6.2099	6.5654	6.9030	8.7430
L/h=20								
0	Vo et al. [3] (HOBT)	12.2228	12.2228	12.2228	12.2228	12.2228	12.2228	12.2228
	Present (Quasi-3D)	12.2660	12.2660	12.2660	12.2660	12.2660	12.2660	12.2660
0.5	Vo et al. [3] (HOBT)	9.6942	9.9501	10.1001	10.1800	10.3668	10.5460	11.4459
	Present (Quasi-3D)	9.7297	9.9865	10.1403	10.2172	10.4072	10.5842	11.4867
1	Vo et al. [3] (HOBT)	8.3594	8.7241	8.9474	9.0722	9.3550	9.6411	11.0421
	Present (Quasi-3D)	8.3908	8.7569	8.9893	9.1061	9.3964	9.6768	11.0815
2	Vo et al. [3] (HOBT)	7.1563	7.5417	7.8293	7.9727	8.3430	8.7262	10.6336
	Present (Quasi-3D)	7.1839	7.5711	7.8753	8.0035	8.3877	8.7593	10.6719
5	Vo et al. [3] (HOBT)	6.4064	6.6116	6.9389	7.0170	7.4461	7.8692	10.2298
	Present (Quasi-3D)	6.4308	6.6379	6.9891	7.0451	7.4955	7.9000	10.2669
10	Vo et al. [3] (HOBT)	6.3086	6.3590	6.6889	6.6924	7.1296	7.5311	10.0519
	Present (Quasi-3D)	6.3319	6.3841	6.7395	6.7194	7.1809	7.5609	10.0884

Table 6: The fundamental natural frequencies of FG sandwich C-F beams (Type A).

k	Theory	1-0-1	2-1-2	2-1-1	1-1-1	2-2-1	1-2-1	1-8-1
L/h=5								
0	Vo et al. [3] (HOBT)	1.8952	1.8952	1.8952	1.8952	1.8952	1.8952	1.8952
	Present (Quasi-3D)	1.9055	1.9055	1.9055	1.9055	1.9055	1.9055	1.9055
0.5	Vo et al. [3] (HOBT)	1.5069	1.5466	1.5696	1.5821	1.6108	1.6384	1.7764
	Present (Quasi-3D)	1.5152	1.5551	1.5787	1.5908	1.6200	1.6474	1.7859
1	Vo et al. [3] (HOBT)	1.3007	1.3575	1.3918	1.4115	1.4549	1.4992	1.7145
	Present (Quasi-3D)	1.3081	1.3652	1.4008	1.4193	1.4640	1.5075	1.7235
2	Vo et al. [3] (HOBT)	1.1143	1.1746	1.2188	1.2416	1.2986	1.3582	1.6518
	Present (Quasi-3D)	1.1208	1.1815	1.2282	1.2488	1.3079	1.3658	1.6605
5	Vo et al. [3] (HOBT)	0.9973	1.0303	1.0806	1.0935	1.1597	1.2257	1.5897
	Present (Quasi-3D)	1.0030	1.0365	1.0904	1.1002	1.1695	1.2329	1.5981
10	Vo et al. [3] (HOBT)	0.9812	0.9909	1.0416	1.0431	1.1106	1.1734	1.5624
	Present (Quasi-3D)	0.9867	0.9969	1.0514	1.0495	1.1206	1.1804	1.5706
L/h=20								
0	Vo et al. [3] (HOBT)	1.9496	1.9496	1.9496	1.9496	1.9496	1.9496	1.9496
	Present (Quasi-3D)	1.9527	1.9527	1.9527	1.9527	1.9527	1.9527	1.9527
0.5	Vo et al. [3] (HOBT)	1.5397	1.5805	1.6048	1.6175	1.6477	1.6766	1.8229
	Present (Quasi-3D)	1.5423	1.5831	1.6081	1.6201	1.6509	1.6794	1.8259
1	Vo et al. [3] (HOBT)	1.3253	1.3831	1.4191	1.4388	1.4844	1.5304	1.7573
	Present (Quasi-3D)	1.3275	1.3855	1.4230	1.4413	1.4881	1.5329	1.7602
2	Vo et al. [3] (HOBT)	1.1330	1.1937	1.2398	1.2623	1.3217	1.3831	1.6911
	Present (Quasi-3D)	1.1351	1.1958	1.2447	1.2646	1.3262	1.3855	1.6938
5	Vo et al. [3] (HOBT)	1.0145	1.0453	1.0977	1.1096	1.1781	1.2456	1.6257
	Present (Quasi-3D)	1.0163	1.0473	1.1036	1.1116	1.1837	1.2478	1.6284
10	Vo et al. [3] (HOBT)	1.0005	1.0053	1.0581	1.0578	1.1276	1.1915	1.5969
	Present (Quasi-3D)	1.0022	1.0072	1.0641	1.0598	1.1336	1.1937	1.5995

Table 7: The critical buckling loads of FG sandwich S-S beams (Type A).

k	Theory	1-0-1	2-1-2	2-1-1	1-1-1	2-2-1	1-2-1	1-8-1
L/h=5								
0	Vo et al. [3] (HOBT)	48.5959	48.5959	48.5959	48.5959	48.5959	48.5959	48.5959
	Present (Quasi-3D)	49.5906	49.5906	49.5906	49.5906	49.5906	49.5906	49.5906
0.5	Vo et al. [3] (HOBT)	27.8574	30.0301	31.0728	31.8784	33.2536	34.7653	41.9897
	Present (Quasi-3D)	28.4624	30.6825	31.7627	32.5699	33.9858	35.5156	42.8751
1	Vo et al. [3] (HOBT)	19.6525	22.2108	23.5246	24.5596	26.3611	28.4447	38.7838
	Present (Quasi-3D)	20.7425	22.7065	24.0838	25.1075	26.9764	29.0755	39.6144
2	Vo et al. [3] (HOBT)	13.5801	15.9152	17.3249	18.3587	20.3750	22.7863	35.6914
	Present (Quasi-3D)	13.8839	16.2761	17.7742	18.7772	20.8879	23.3042	36.4677
5	Vo et al. [3] (HOBT)	10.1460	11.6676	13.0270	13.7212	15.7307	18.0914	32.7725
	Present (Quasi-3D)	10.3673	11.9301	13.3924	14.0353	16.1605	18.5092	33.4958
10	Vo et al. [3] (HOBT)	9.4515	10.5348	11.8370	12.2605	14.1995	16.3783	31.5265
	Present (Quasi-3D)	9.6535	10.7689	12.1737	12.5393	14.5994	16.7574	32.2264
L/h=20								
0	Vo et al. [3] (HOBT)	53.2364	53.2364	53.2364	53.2364	53.2364	53.2364	53.2364
	Present (Quasi-3D)	53.3145	53.3145	53.3145	53.3145	53.3145	53.3145	53.3145
0.5	Vo et al. [3] (HOBT)	29.7175	32.2629	33.2376	34.0862	35.6405	37.3159	45.5742
	Present (Quasi-3D)	29.7626	32.1022	33.3127	34.1380	35.7149	41.8227	45.6424
1	Vo et al. [3] (HOBT)	20.7212	23.4211	24.8796	25.9588	27.9540	30.2307	41.9004
	Present (Quasi-3D)	20.7530	23.4572	24.9697	25.9989	28.0412	30.2774	41.9639
2	Vo et al. [3] (HOBT)	14.1973	16.6050	18.1404	19.3116	21.3927	23.9900	38.3831
	Present (Quasi-3D)	14.2190	16.6307	18.2493	19.2299	21.4986	24.0276	38.4419
5	Vo et al. [3] (HOBT)	10.6171	12.0883	13.5523	14.2284	16.3834	18.8874	35.0856
	Present (Quasi-3D)	10.6330	12.1068	13.6717	14.2505	16.5069	18.9172	35.1400
10	Vo et al. [3] (HOBT)	9.9847	10.9075	12.3084	12.6819	14.7525	17.0443	33.6843
	Present (Quasi-3D)	9.9995	10.9239	12.4256	12.7014	14.8807	17.0712	33.7367

Table 8: The critical buckling loads of FG sandwich C-C beams (Type A).

k	Theory	1-0-1	2-1-2	2-1-1	1-1-1	2-2-1	1-2-1	1-8-1
L/h=5								
0	Vo et al. [3] (HOBT)	152.1470	152.1470	152.1470	152.1470	152.1470	152.1470	152.1470
	Present (Quasi-3D)	160.2780	160.2780	160.2780	160.2780	160.2780	160.2780	160.2780
0.5	Vo et al. [3] (HOBT)	92.8833	99.9860	102.9120	105.6790	109.6030	114.1710	134.2870
	Present (Quasi-3D)	98.4559	105.9750	109.0360	111.9680	116.0700	120.8630	141.7880
1	Vo et al. [3] (HOBT)	67.4983	76.2634	80.1670	83.8177	89.2208	95.7287	125.3860
	Present (Quasi-3D)	71.7654	81.0936	85.2092	89.0834	94.7675	101.6130	132.5510
2	Vo et al. [3] (HOBT)	47.7010	56.2057	60.6056	64.4229	70.7563	78.5608	116.6580
	Present (Quasi-3D)	50.8183	59.9354	64.6133	68.6743	75.3818	83.6159	123.4770
5	Vo et al. [3] (HOBT)	35.5493	42.0033	46.3743	49.2763	55.8271	63.7824	108.2970
	Present (Quasi-3D)	37.8295	44.8488	49.5325	52.6395	59.6248	68.0510	114.7700
10	Vo et al. [3] (HOBT)	32.3019	37.9944	42.1935	44.3374	50.7315	58.2461	104.6920
	Present (Quasi-3D)	34.2824	40.5544	45.0660	47.3804	54.2193	62.1959	111.0120
L/h=20								
0	Vo et al. [3] (HOBT)	208.9510	208.9510	208.9510	208.9510	208.9510	208.9510	208.9510
	Present (Quasi-3D)	210.7420	210.7420	210.7420	210.7420	210.7420	210.7420	210.7420
0.5	Vo et al. [3] (HOBT)	117.3030	126.5080	131.1240	134.4810	140.5450	147.1040	179.2350
	Present (Quasi-3D)	118.3530	127.6410	132.3830	135.6840	141.8690	148.4130	180.8010
1	Vo et al. [3] (HOBT)	81.9927	92.6741	98.3880	102.6650	110.4830	119.4220	164.9490
	Present (Quasi-3D)	82.7434	93.5248	99.4730	103.6060	111.6480	120.5090	166.4060
2	Vo et al. [3] (HOBT)	56.2773	65.8489	71.8900	76.1020	84.7291	94.9563	151.2500
	Present (Quasi-3D)	56.7986	66.4664	72.8506	76.8166	85.7783	95.8403	152.6000
5	Vo et al. [3] (HOBT)	42.0775	48.0070	53.7820	56.4958	65.0007	74.8903	138.3880
	Present (Quasi-3D)	42.4596	48.4588	54.6418	57.0343	65.9671	75.6019	139.6370
10	Vo et al. [3] (HOBT)	39.4930	43.3233	48.8510	50.3811	58.5607	67.6270	132.9170
	Present (Quasi-3D)	39.8436	43.7273	49.6622	50.8611	59.4944	68.2737	134.1220

Table 9: The critical buckling loads of FG sandwich C-F beams (Type A).

k	Theory	1-0-1	2-1-2	2-1-1	1-1-1	2-2-1	1-2-1	1-8-1
L/h=5								
0	Vo et al. [3] (HOBT)	13.0594	13.0594	13.0594	13.0594	13.0594	13.0594	13.0594
	Present (Quasi-3D)	13.1224	13.1224	13.1224	13.1224	13.1224	13.1224	13.1224
0.5	Vo et al. [3] (HOBT)	7.3314	7.9068	8.1951	8.4051	8.7839	9.1940	11.2021
	Present (Quasi-3D)	7.3700	7.9482	8.2431	8.4486	8.8334	9.2404	11.2557
1	Vo et al. [3] (HOBT)	5.1245	5.7921	6.1490	6.4166	6.9050	7.4639	10.3093
	Present (Quasi-3D)	5.1533	5.8244	6.1944	6.4516	6.9518	7.5028	10.3581
2	Vo et al. [3] (HOBT)	3.5173	4.1156	4.4927	4.7564	5.2952	5.9348	9.4531
	Present (Quasi-3D)	3.5387	4.1408	4.5376	4.7847	5.3419	5.9674	9.4974
5	Vo et al. [3] (HOBT)	2.6298	3.0004	3.3609	3.5310	4.0620	4.6806	8.6493
	Present (Quasi-3D)	2.6458	3.0203	3.4046	3.5542	4.1095	4.7088	8.6897
10	Vo et al. [3] (HOBT)	2.4683	2.7077	3.0527	3.1488	3.6595	4.2267	8.3073
	Present (Quasi-3D)	2.4823	2.7257	3.0946	3.1702	3.7068	4.2533	8.3463
L/h=20								
0	Vo et al. [3] (HOBT)	13.3730	13.3730	13.3730	13.3730	13.3730	13.3730	13.3730
	Present (Quasi-3D)	13.3981	13.3981	13.3981	13.3981	13.3981	13.3981	13.3981
0.5	Vo et al. [3] (HOBT)	7.4543	8.0405	8.3385	8.5512	8.9422	9.3634	11.4424
	Present (Quasi-3D)	7.4689	8.0563	8.3609	8.5679	8.9647	9.3815	11.4642
1	Vo et al. [3] (HOBT)	5.1944	5.8713	6.2378	6.5083	7.0096	7.5815	10.5174
	Present (Quasi-3D)	5.2050	5.8832	6.2633	6.5214	7.0346	7.5965	10.5375
2	Vo et al. [3] (HOBT)	3.5574	4.1603	4.5457	4.8110	5.3615	6.0134	9.6321
	Present (Quasi-3D)	3.5648	4.1690	4.5753	4.8211	5.3906	6.0257	9.6507
5	Vo et al. [3] (HOBT)	2.6605	3.0275	3.3948	3.5637	4.1043	4.7323	8.8025
	Present (Quasi-3D)	2.6659	3.0341	3.4266	3.5714	4.1373	4.7423	8.8196
10	Vo et al. [3] (HOBT)	2.5032	2.7317	3.0832	3.1759	3.6952	4.2698	8.4500
	Present (Quasi-3D)	2.5082	2.7376	3.1142	3.1829	3.7293	4.2789	8.4666

Table 10: The fundamental natural frequencies of (1-8-1) FG sandwich beams (Type B).

BC	Reference	k = 0	k = 0.5	k = 1	k = 2	k = 5	k = 10
L/h=5							
C-C	Present (HOBT)	9.3088	8.3073	7.7343	7.1818	6.6832	6.4634
	Present (Quasi-3D)	9.4258	8.4380	7.8723	7.3193	6.8019	6.5661
S-S	Present (HOBT)	4.6694	4.1201	3.8243	3.5777	3.4474	3.4204
	Present (Quasi-3D)	4.6829	4.1538	3.8708	3.6331	3.5011	3.4671
C-F	Present (HOBT)	1.7116	1.5138	1.4101	1.3272	1.2907	1.2856
	Present (Quasi-3D)	1.7223	1.5303	1.4302	1.3497	1.3124	1.3050
L/h=20							
C-C	Present (HOBT)	11.0234	9.7510	9.0879	8.5646	8.3521	8.3323
	Present (Quasi-3D)	11.0730	9.8405	9.2030	8.6978	8.4814	8.4466
S-S	Present (HOBT)	4.9141	4.3424	4.0462	3.8166	3.7363	3.7387
	Present (Quasi-3D)	4.9196	4.3697	4.0874	3.8679	3.7871	3.7825
C-F	Present (HOBT)	1.7541	1.5502	1.4448	1.3634	1.3357	1.3370
	Present (Quasi-3D)	1.7586	1.5620	1.4612	1.3831	1.3551	1.3541

Table 11: The critical buckling loads of (1-8-1) FG sandwich beams (Type B).

BC	Reference	k = 0	k = 0.5	k = 1	k = 2	k = 5	k = 10
L/h=5							
C-C	Present (HOBT)	125.3150	90.9406	75.1345	61.7804	51.1263	46.8477
	Present (Quasi-3D)	132.5240	96.3946	79.7050	65.4693	53.8798	49.1767
S-S	Present (HOBT)	38.6762	27.7155	22.9142	19.2140	20.8604	16.2077
	Present (Quasi-3D)	39.5558	28.5495	23.7280	19.9763	17.6062	16.7752
C-F	Present (HOBT)	10.2735	7.3321	6.0634	5.1174	4.6179	4.4854
	Present (Quasi-3D)	10.3433	7.4536	6.2077	5.2690	4.7526	4.5989
L/h=20							
C-C	Present (HOBT)	164.3840	117.3430	97.0548	81.9222	73.9263	71.8001
	Present (Quasi-3D)	166.1240	119.6690	99.6524	84.5833	76.3160	73.8660
S-S	Present (HOBT)	41.7477	29.7636	24.6163	20.8127	18.8976	18.4377
	Present (Quasi-3D)	41.8917	30.1685	25.1407	21.3901	19.4285	18.8840
C-F	Present (HOBT)	10.4785	7.4681	6.1765	5.2244	4.7512	4.6410
	Present (Quasi-3D)	10.5189	7.5729	6.3107	5.3715	4.8858	4.7553

Table 12: The first four natural frequencies of (2-1-1) FG sandwich beams (Type A, L/h=5).

BC	k	Present (HOBT)				Present (Quasi-3D)			
		ω_1	ω_2	ω_3	ω_4	ω_1	ω_2	ω_3	ω_4
C-C	0	10.0678	24.1007	30.2391	39.0057	10.1851	24.3924	31.6992	39.3368
	0.5	8.6673	21.1460	28.1189	34.8381	8.7755	21.4361	29.4679	35.2373
	1	7.8390	19.3241	26.8406	32.1979	7.9431	19.6136	28.1134	32.6359
	2	6.9908	17.4038	25.3680	29.3500	7.0920	17.6906	26.5466	29.8151
	5	6.2737	15.7219	23.6440	26.7525	6.3718	15.9981	24.7160	27.2129
	10	6.0527	15.1729	22.7555	25.8348	6.1485	15.4403	23.7804	26.2779
S-S	0	5.1528	15.1167	17.8812	34.2097	5.1618	15.8466	17.9788	34.5180
	0.5	4.2945	14.0135	15.3114	29.8664	4.3041	14.6649	15.4305	30.1902
	1	3.8187	13.2067	13.9412	27.2035	3.8301	13.6220	14.2601	27.5384
	2	3.3514	11.9476	12.8895	24.4133	3.3656	12.1562	13.3684	24.7516
	5	2.9746	10.6864	11.9590	21.9917	2.9912	10.8591	12.4142	22.3149
	10	2.8669	10.2784	11.5216	21.2123	2.8839	10.4519	11.9469	21.5226
C-F	0	1.8952	10.2454	15.1167	24.4965	1.9055	10.3171	15.8466	24.6877
	0.5	1.5696	8.7177	14.0573	21.2776	1.5787	8.7849	14.7305	21.4777
	1	1.3918	7.8330	13.4191	19.3337	1.4008	7.8997	14.0524	19.5406
	2	1.2188	6.9394	12.6837	17.3116	1.2282	7.0069	13.2670	17.5233
	5	1.0806	6.1960	11.8227	15.5670	1.0904	6.2641	12.3495	15.7757
	10	1.0416	5.9730	11.3790	15.0115	1.0514	6.0402	11.8817	15.2144

Table 13: The first four natural frequencies of (2-1-1) FG sandwich beams (Type B, L/h=5).

BC	k	Present (HOBT)				Present (Quasi-3D)			
		ω_1	ω_2	ω_3	ω_4	ω_1	ω_2	ω_3	ω_4
C-C	0	7.2279	17.7376	25.3767	29.4689	7.3870	18.1654	26.2069	30.1539
	0.5	7.0660	17.1549	24.2580	28.1654	7.2195	17.5634	25.0301	28.8006
	1	6.9690	16.8056	23.6490	27.4000	7.1178	17.1979	24.3953	27.9992
	2	6.8606	16.4138	23.0024	26.5560	7.0028	16.7837	23.7274	27.1103
	5	6.7424	15.9865	22.3143	25.6550	6.8757	16.3271	23.0254	26.1552
	10	6.6878	15.7897	21.9867	25.2472	6.8163	16.1149	22.6948	25.7203
S-S	0	3.4836	11.0242	13.7319	24.8211	3.5478	11.3936	14.0025	25.4339
	0.5	3.4573	10.5981	13.3462	24.0449	3.5233	10.9607	13.5995	24.6515
	1	3.4460	10.3751	13.1275	23.5889	3.5122	10.7327	13.3717	24.1828
	2	3.4381	10.1508	12.8888	23.0846	3.5037	10.5031	13.1228	23.6561
	5	3.4356	9.9316	12.6317	22.5420	3.4993	10.2789	12.8531	23.0787
	10	3.4364	9.8359	12.5115	22.2942	3.4988	10.1816	12.7261	22.8105
C-F	0	1.2857	7.1612	12.7211	17.6159	1.3111	7.3119	13.0913	18.0167
	0.5	1.2823	7.0340	12.1694	17.1120	1.3082	7.1843	12.5099	17.5046
	1	1.2819	6.9619	11.8686	16.8190	1.3078	7.1102	12.1959	17.2019
	2	1.2833	6.8854	11.5485	16.4990	1.3090	7.0300	11.8649	16.8666
	5	1.2870	6.8070	11.2066	16.1604	1.3120	6.9455	11.5164	16.5055
	10	1.2894	6.7725	11.0435	16.0077	1.3140	6.9071	11.3524	16.3400

CAPTIONS OF FIGURES

Figure 1: Geometry and coordinate of a FG sandwich beam.
Figure 2: Buckling mode shapes of (1-8-1) clamped- clamped FG sandwich beam (Type B, L/h=5) using HOBT and quasi-3D theory.
Figure 3: Fundamental natural frequencies and critical buckling loads of (1-0-1) and (1-8-1) simply-supported FG sandwich beams (Type A).
Figure 4: Vibration mode shapes of (2-1-1) simply-supported FG sandwich beam (Type A, k=1, L/h=5) using HOBT and quasi-3D theory.
Figure 5: Vibration mode shapes of (2-1-1) simply-supported FG sandwich beam (Type B, k=1, L/h=5) using HOBT and quasi-3D theory.

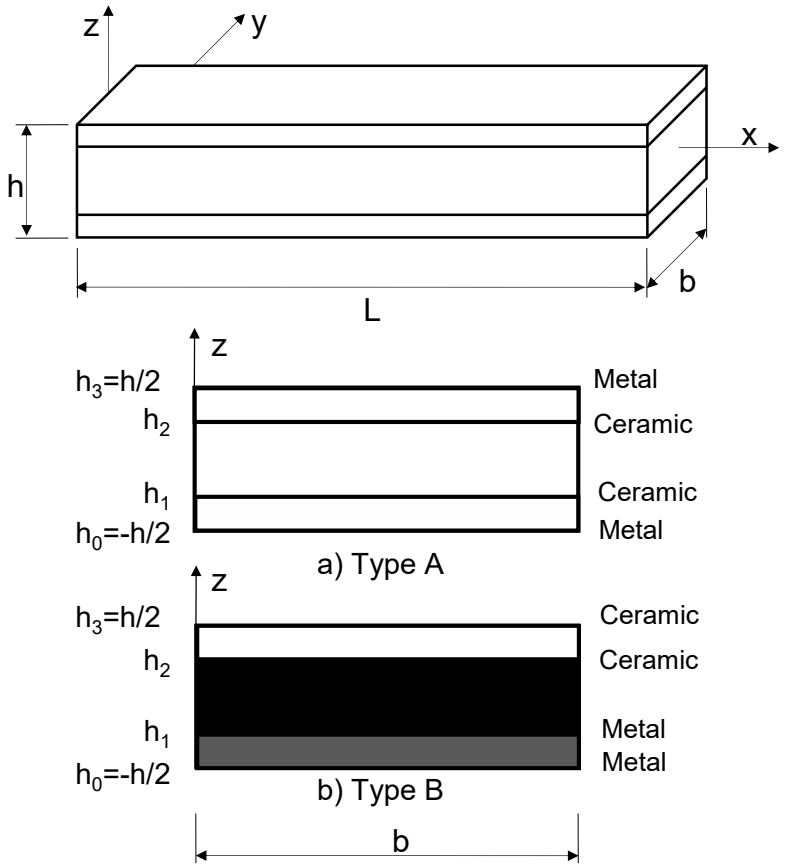

Figure 1: Geometry and coordinate of a FG sandwich beam.

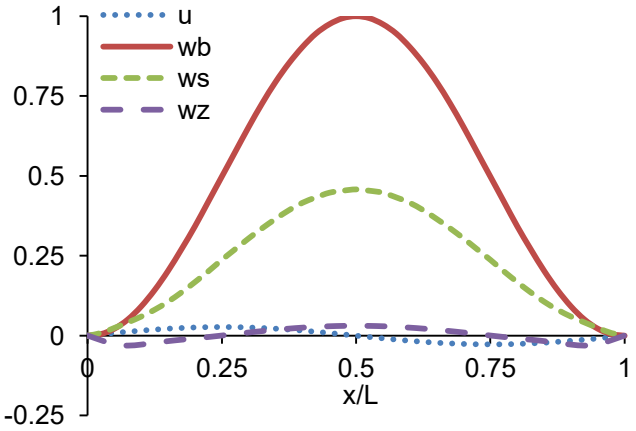

a.P_{cr}= 132.5240 (k=0)

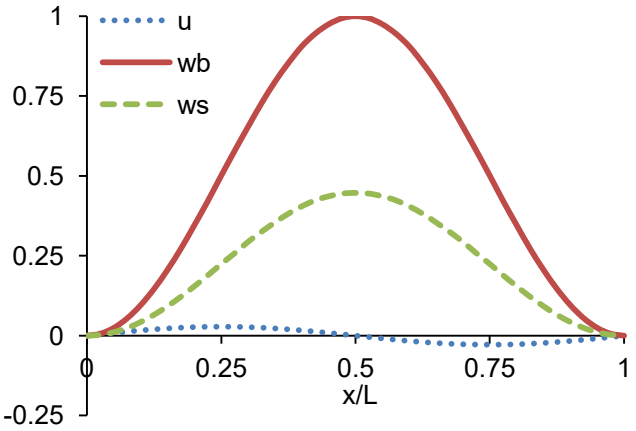

a. P_{cr}= 125.3150 (k=0)

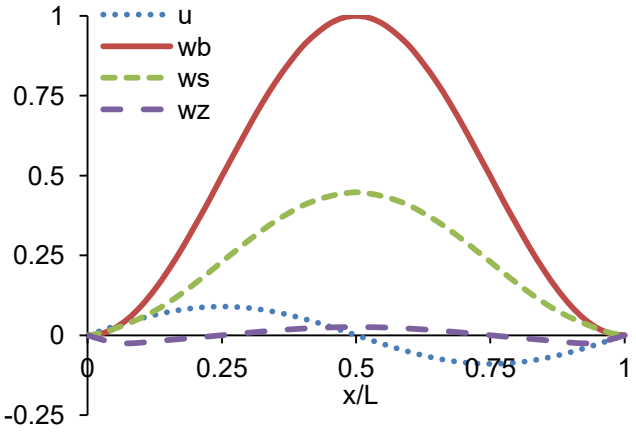

b. P_{cr}= 79.7050 (k=1)

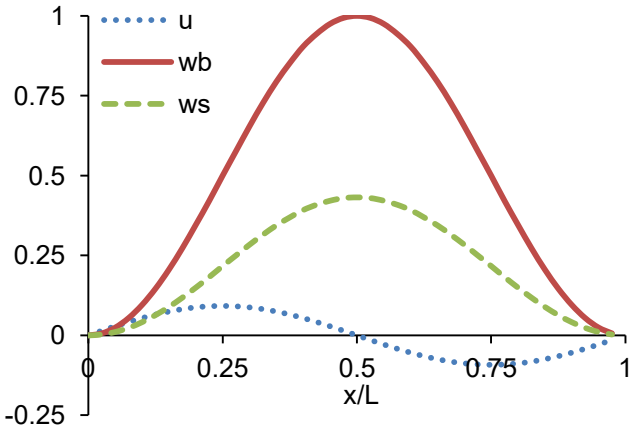

b. P_{cr}= 75.1345 (k=1)

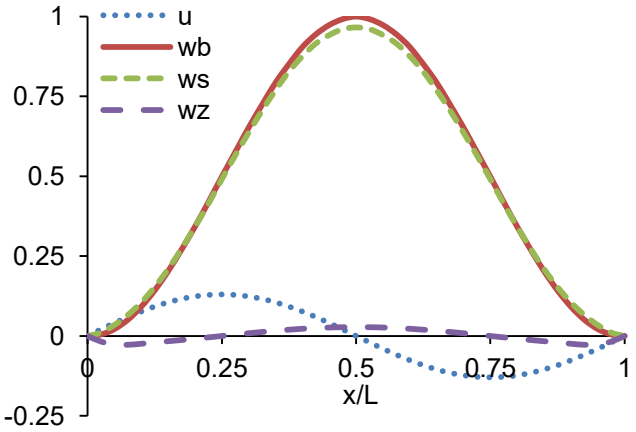

c. P_{cr}= 49.1767 (k=10)

Present (Quasi-3D)

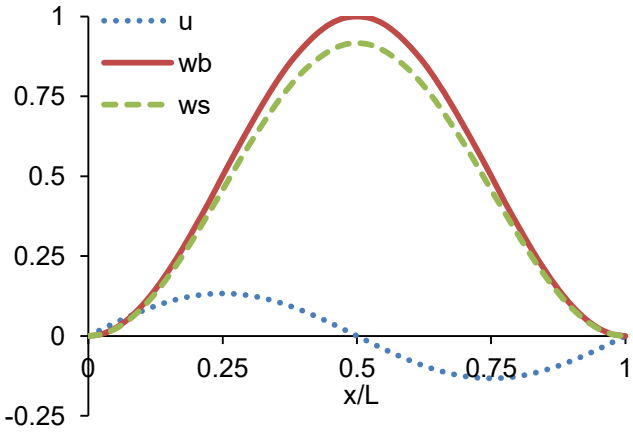

c. P_{cr}= 46.8477 (k=10)

Present (HOBT)

Figure 2: Buckling mode shapes of (1-8-1) clamped- clamped FG sandwich beam (Type B, L/h=5) using HOBT and quasi-3D theory.

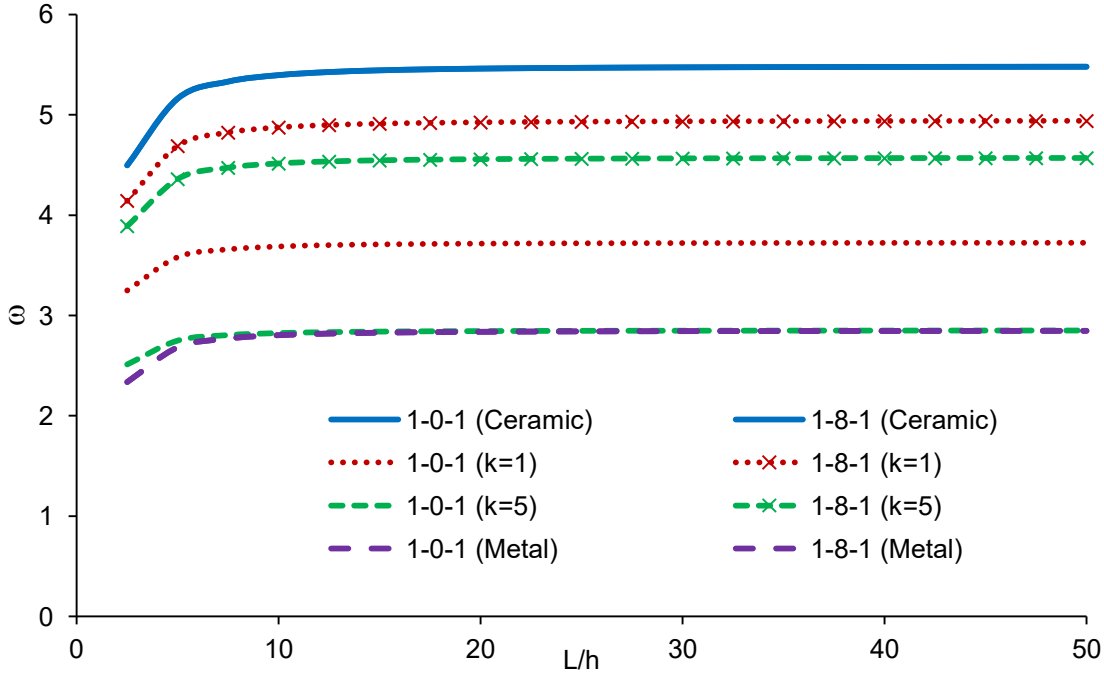

a. Fundamental natural frequencies

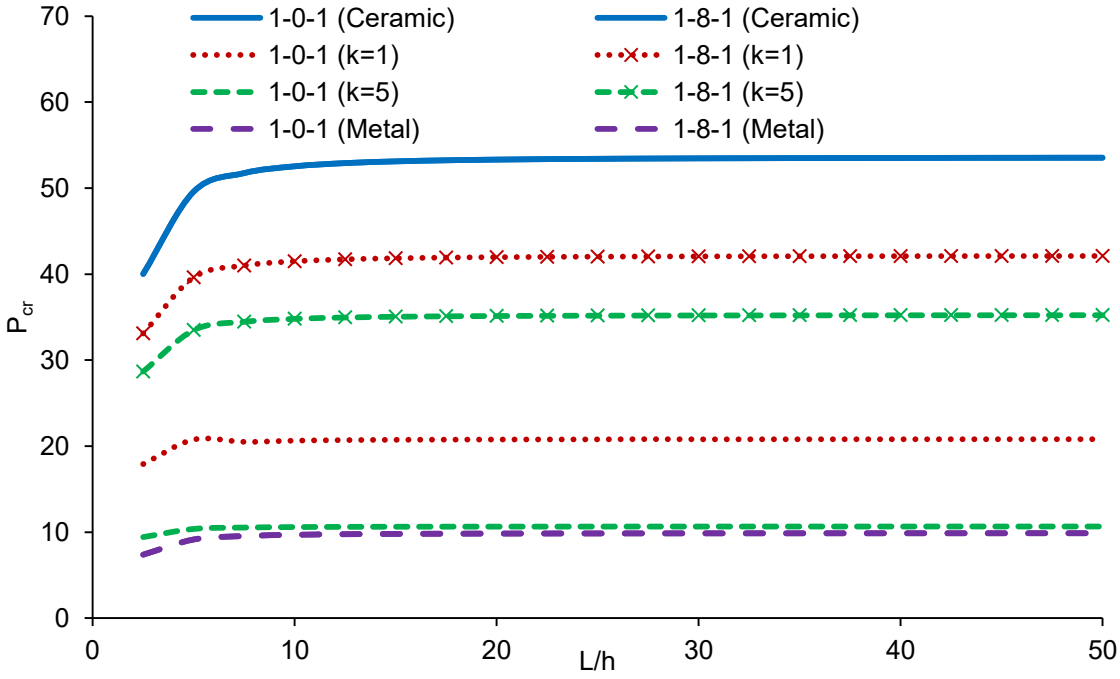

b. Critical buckling loads

Figure 3: Fundamental natural frequencies and critical buckling loads of (1-0-1) and (1-8-1) simply-supported FG sandwich beams (Type A).

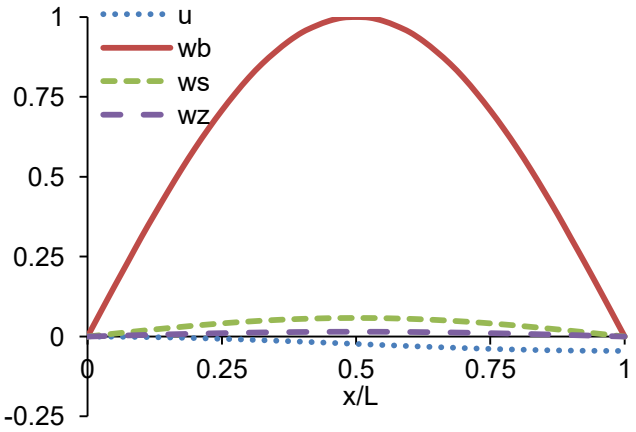

a. First mode $\omega_1 = 3.8301$

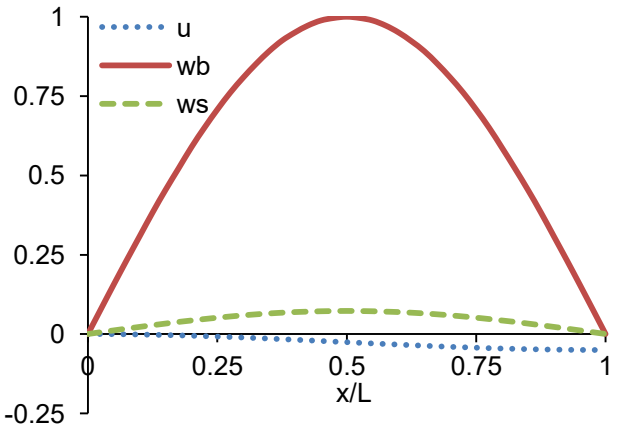

a. First mode $\omega_1 = 3.8187$

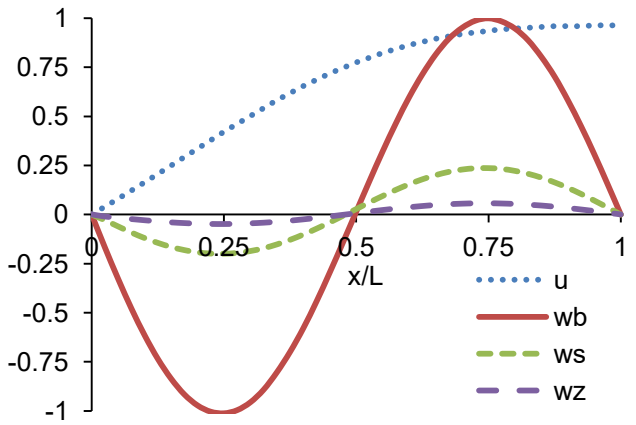

b. Second mode $\omega_2 = 13.6220$

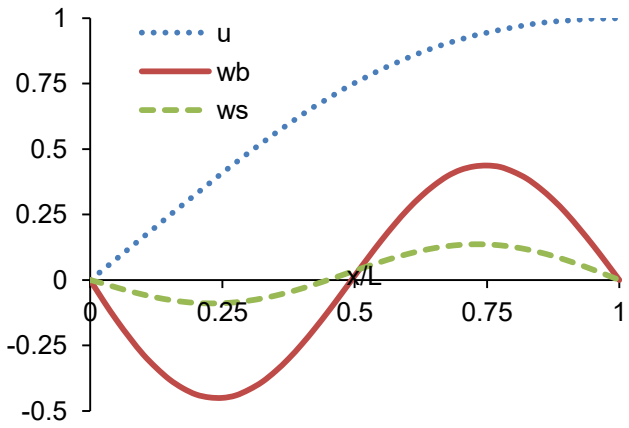

b. Second mode $\omega_2 = 13.2067$

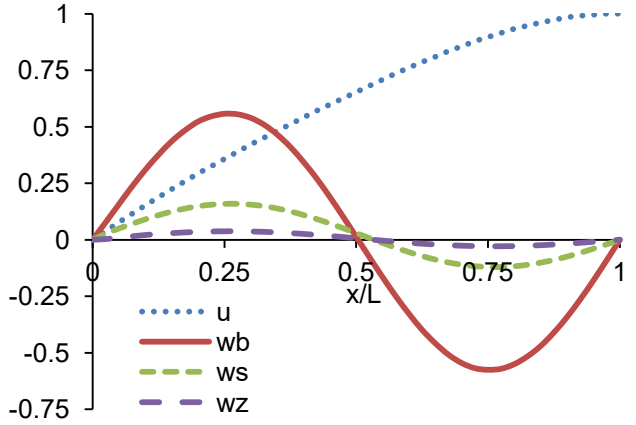

c. Third mode $\omega_3 = 14.2601$

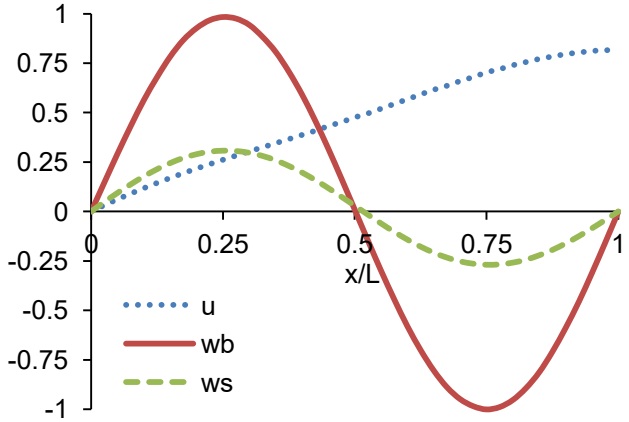

c. Third mode $\omega_3 = 13.9412$

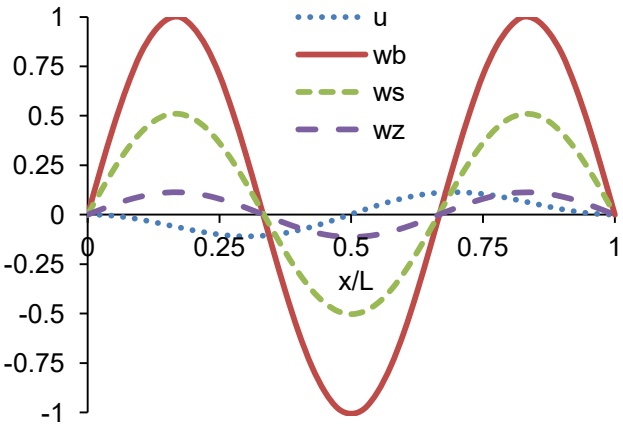

d. Fourth mode $\omega_4 = 27.5384$

Present (Quasi-3D)

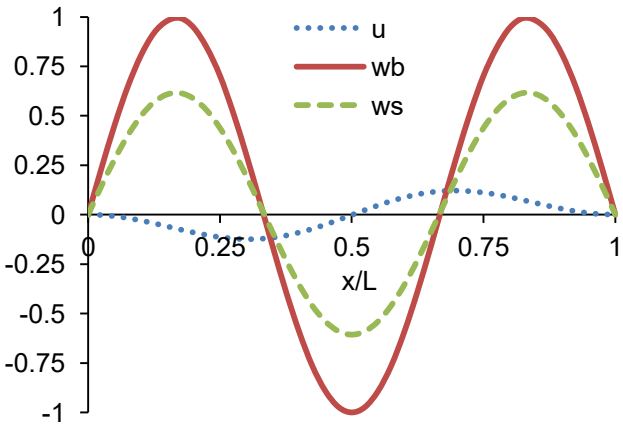

d. Fourth mode $\omega_4 = 27.2035$

Present (HOBT)

Figure 4: Vibration mode shapes of (2-1-1) simply-supported FG sandwich beam (Type A, k=1, L/h=5) using HOBT and quasi-3D theory.

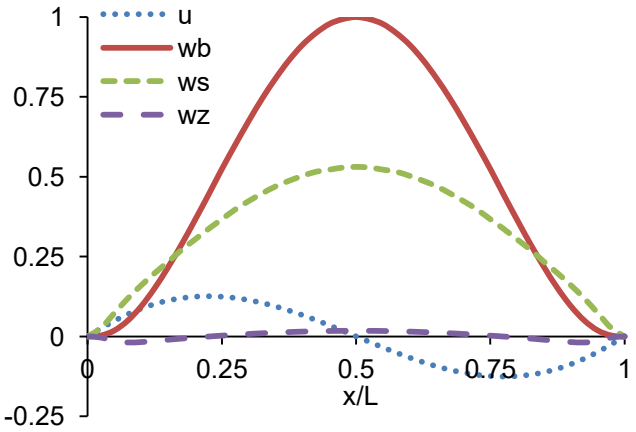

a. First mode ω_1 = 7.1178

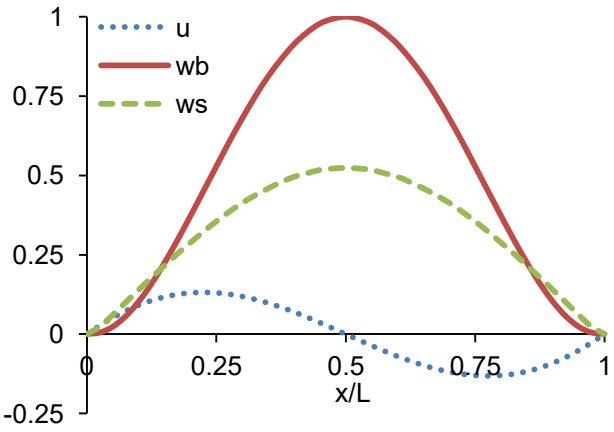

a. First mode ω_1 =6.9690

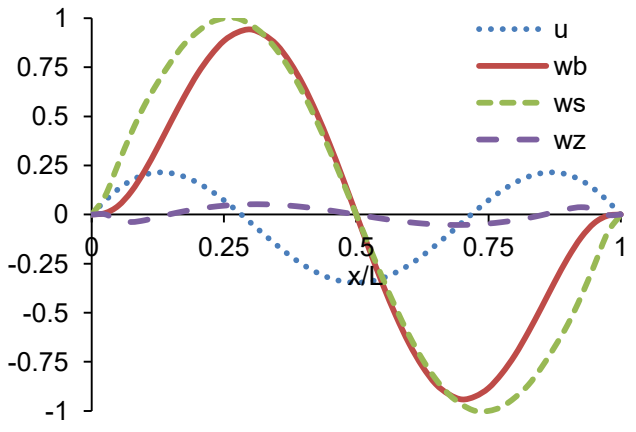

b. Second mode ω_2 = 17.1979

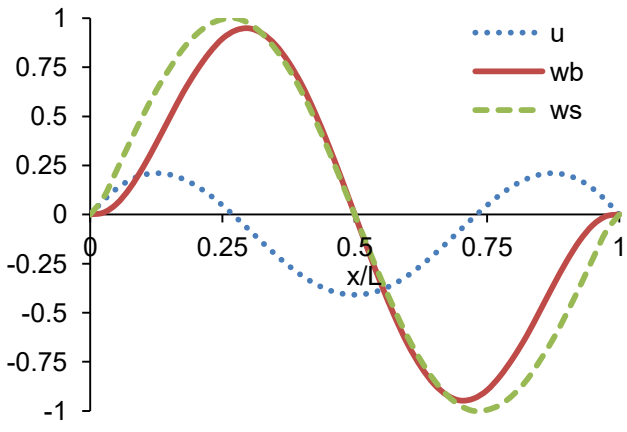

b. Second mode ω_2 = 16.8056

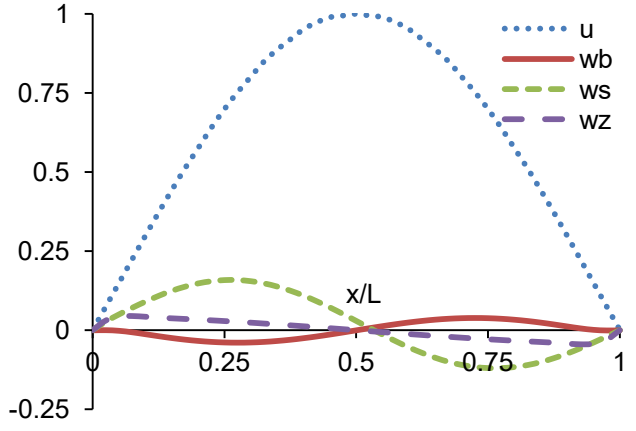

c. Third mode ω_3 = 24.3953

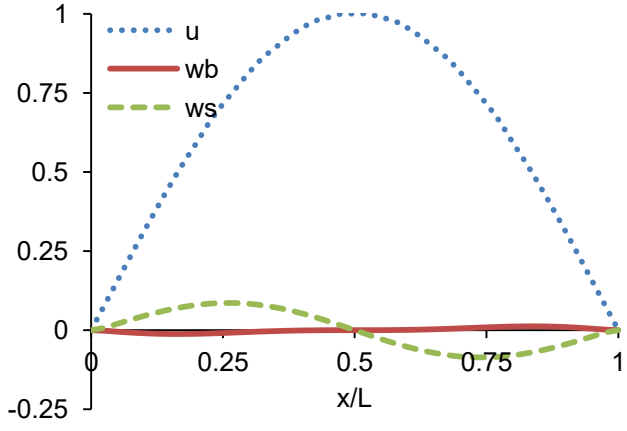

c. Third mode ω_3 = 23.6490

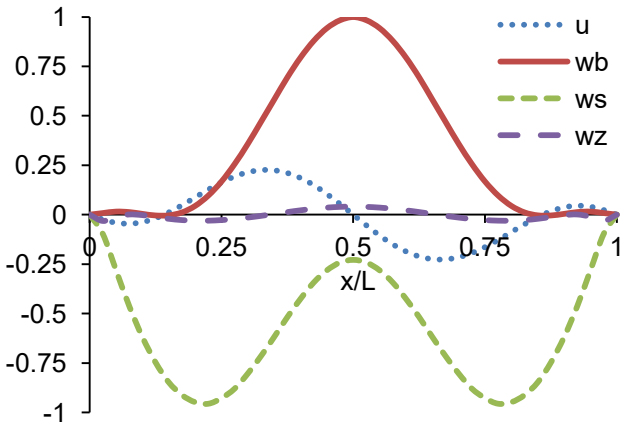

d. Fourth mode $\omega_4 = 27.9992$

Present (Quasi-3D)

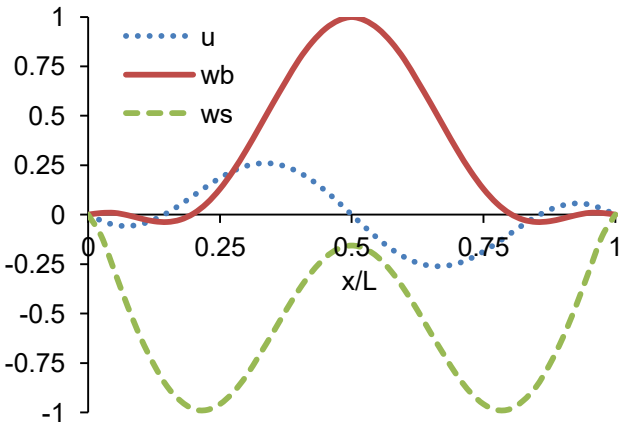

d. Fourth mode $\omega_4 = 27.4000$

Present (HOBT)

Figure 5: Vibration mode shapes of (2-1-1) simply-supported FG sandwich beam (Type B, k=1, L/h=5) using HOBT and quasi-3D theory.